

Comparison of open-source image-based reconstruction pipelines for 3D root phenotyping of field-grown maize

Suxing Liu^{a,b,c}, Wesley Paul Bonelli^a, Peter Pietrzik^a, Alexander Bucksch^{a,b,c}

^aDepartment of Plant Biology, University of Georgia, Athens, GA, USA, 30605.

^bWarnell School of Forestry and Natural Resources, University of Georgia, Athens, GA, USA, 30605.

^cInstitute of Bioinformatics, University of Georgia, Athens, GA, USA, 30605.

ABSTRACT

Understanding root traits is essential to improve water uptake, increase nitrogen capture and accelerate carbon sequestration from the atmosphere. High-throughput phenotyping to quantify root traits for deeper field-grown roots remains a challenge, however. Recently developed open-source methods use 3D reconstruction algorithms to build 3D models of plant roots from multiple 2D images and can extract root traits and phenotypes. Most of these methods rely on automated image orientation (Structure from Motion)[1] and dense image matching (Multiple View Stereo) algorithms to produce a 3D point cloud or mesh model from 2D images. Until now the performance of these methods when applied to field-grown roots has not been compared tested commonly used open-source pipelines on a test panel of twelve contrasting maize genotypes grown in real field conditions[2-6]. We compare the 3D point clouds produced in terms of number of points, computation time and model surface density. This comparison study provides insight into the performance of different open-source pipelines for maize root phenotyping and illuminates trade-offs between 3D model quality and performance cost for future high-throughput 3D root phenotyping.

Keywords: 3D reconstruction, maize roots, 3D point cloud

1. INTRODUCTION

Root phenotyping is essential to improve water uptake, nitrogen capture and carbon sequestration[7] [8-12], but requires advanced methods to measure and quantify complex root architectures. With the development of computer vision techniques, image-based root phenotyping with commodity cameras has emerged as a cost efficient and accessible alternative to high-end imaging devices.

Established 2D image-based root phenotyping methods provide abundant trait measurements [13]. Examples include DIRT [14], archiDART [15], EZ-Root-VIS [16], GiA Roots [17] and RhizoVision [18]. 2D imaging approaches can only capture partial information from dense and highly occluded 3D maize root structures, however. As such, quantifying important traits such as crown root number and whorl number and the distance remains challenging [19].

3D phenotyping methods are a promising option thanks to their ability to leverage multiple views of a given scene to resolve highly occluded structures [20] [21-23]. One of the key challenges in 3D root phenotyping method is to reconstruct a 3D representation of the root [19]. The available open-source image-based 3D

reconstruction pipelines can process large sets of unordered and diverse images and generate a dense colored point cloud model or a triangulated textured mesh [24]. However, the performance of each pipeline varies dependent on the computing environment and the complexity of the object to be reconstructed. Here we attempt to determine the suitability of available reconstruction pipelines for efficiently producing high-quality models of field-grown maize root systems.

In this study, we compare commonly used open-source 3D reconstruction pipelines on a test panel of twelve contrasting genotypes of field-grown maize roots. These methods include COLMAP [1] [2], VisualSFM [3], OpenMVG [4], Meshroom [5] and Multi-View Environment (MVE) [6]. We compare the resulting point cloud models on measures of visual quality, number and density of points, and computation time.

2. MATERIAL AND METHODS

2.1 Image dataset

Plants were grown at The Pennsylvania State University's Russell E. Larson Agricultural Research Center ($40^{\circ} 42'40.915''$ N, $77^{\circ} 57'11.120''$ W), characterized by a Hagerstown silt loam soil (fine, mixed, semi-active, mesic Typic Hapludalf). Twelve genotypes were selected, including six inbred lines (B101, B112, DKIB014, LH123HT, Pa762, PHZ51) and six hybrid lines (DKPB80 x 3IIH6, H96 x 3IIH6, LH59 x PHG29, Pa762 x 3IIH6, PHG50 x PHG47, PHZ51 x LH59). These genotypes represent the extremes of dense vs. sparse, large vs. small, and maximum and minimum number of whorls selected from a full diversity panel published in Ref. [7]. We selected one plant from each genotype for this initial comparison, yielding 12 total root samples.

We captured images of each root sample with a prototype imaging chamber conceptually introduced in [25] (Fig. 1). Images were captured by ten cameras (Image Source DFK 33ux183 USB 3.0, 12mm focal length V1228-MPY2 12 Megapixel Machine Vision Lens) arrayed around a central focal point. Image capture is synchronized by a cluster of ten Raspberry Pi 4's using a server-client design. For each sample, between 301 and 360 images with image resolution $5,472 \times 3,648$ were captured using a manual rotation stand. Sample images for each genotype are shown in Figure 1.



Figure 1. 3D root imaging chamber.

2.2 Methods

We tested the performance of the pipelines alone and in a number of combinations, including COLMAP, COLMAP+PMVS (Patch-based Multi-view Stereo), VisualSFM, Meshroom and OpenMVG+MVE [1, 2, 6, 24, 26-35]. 3D root models were computed by the five different pipelines on a Dell Workstation. (OptiPlex 7080, 10th Generation Intel® Core™ i9-10900K, 20 MB Cache, 10 Cores, 20 Threads, 3.7 GHz to 5.3 GHz, 125 W, 64 GB RAM, 4 x 16 GB, DDR4, M.2 2280, 1 TB hard drive, Gen 3 PCIe x4 NVMe, Class 40 SSD). In addition, we use a GPU to facilitate the computation when supported by the pipeline. The GPU model installed on the DELL workstation is (GeForce RTX 2070 SUPER, NVIDIA Corporation TU104, nvcc: NVIDIA (R) Cuda compiler driver).

3. RESULTS AND DISCUSSION

We compare the performance of five 3D reconstruction pipelines and combinations thereof. The tested pipelines include COLMAP, COLMAP+PMVS (Patch-based Multi-view Stereo), VisualSFM, Meshroom and OpenMVG+MVE. Overall, we computed 60 point cloud models of the field-grown maize roots.

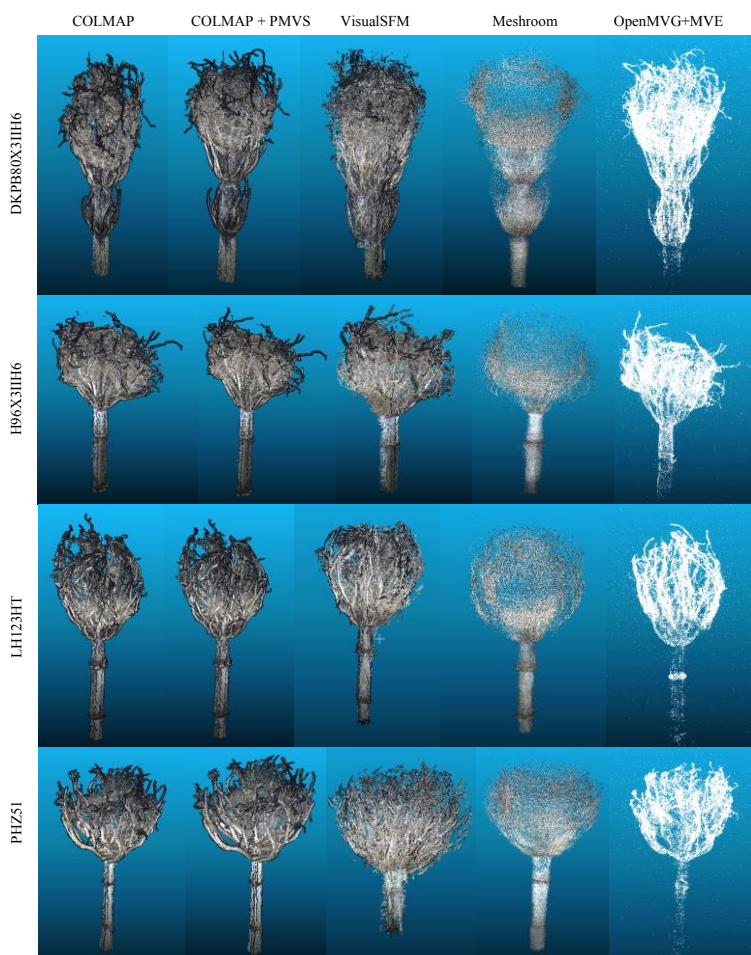


Figure 2. Visual comparison of four genotypes of models

runtimes similar to VisualSFM. We used CloudCompare [36] to load each point cloud model and record its number of points (via a feature in the web UI's "Properties" tab). We also use another tool provided by CloudCompare for computing geometric features to estimate the surface density of the point cloud models. Surface density is defined here as the number of neighbors within a spherical neighborhood of radius R , divided by the neighborhood surface = $N / (\pi \cdot R^2)$. We use the constant $R = 0.005118$ to compute the surface density for each model. The comparison of number of points and surface density are shown in Figure 3 and 4 respectively. COLMAP and OpenMVG+MVE produced the largest point sets, achieving on average 94 and 49 times the number of points of Meshroom respectively. Meshroom produced the smallest point clouds. COLMAP+PMVS and VisualSFM averaged 14 and 9 times more points than Meshroom, respectively. COLMAP and VisualSFM produced models with the greatest surface density: COLMAP, OpenMVG+MVE, COLMAP+PMVS and Meshroom achieves 94, 31, 14, 8 times of VisualSFM in average. COLMAP+PMVS required

We selected four genotypes for a qualitative visual inspection and comparison (Figure 2). COLMAP and COLMAP+PMVS both achieve good quality, including good model completeness (high connectedness of interior points). VisualSFM tended to lose fine details at the margins due to the limited number of input images. Meshroom tended to produce models with large interior gaps. OpenMVG+MVE tended to capture more fine details than VisualSFM, but does not store point color information.

In addition to a qualitative visual inspection, we compare all sixty 3D root models by computing the total number of points and surface density, as well as the recording computation time cost, as shown in Figure 3. On average, COLMAP consumed almost 29-fold the average time of OpenMVG+MVE (5 times that of Meshroom), while COLMAP+PMVS (substituting PMVS for the dense reconstruction step) was significantly faster, consuming only 3 times that of OpenMVG+MVE in average.

4. CONCLUSION

By comparing the performance of all the 3D reconstruction pipelines and its combination in this study, we found out that COLMAP, COLMAP+PMVS and VisualSFM are the three pipelines which can generate

colored 3d root models directly. Although the computation time of COLMAP is 12-times slower than the VisualSFM, COLMAP achieved 10 times greater number of points, and a 94 times higher surface density in our test dataset. A combination of COLMAP+PMVS resulted in similar computation time with VisualSFM, but the model quality achieved 2 and 14 times of VisualSFM in term of number of points and surface density.

Our initial study is a good indicator, however further experiments are needed evaluate the quality of root traits and whole root descriptors to a manually measured ground-truth for a larger amount of 3D models. In that way, we will gain insight into the dependency of trait measurements on method accuracy.

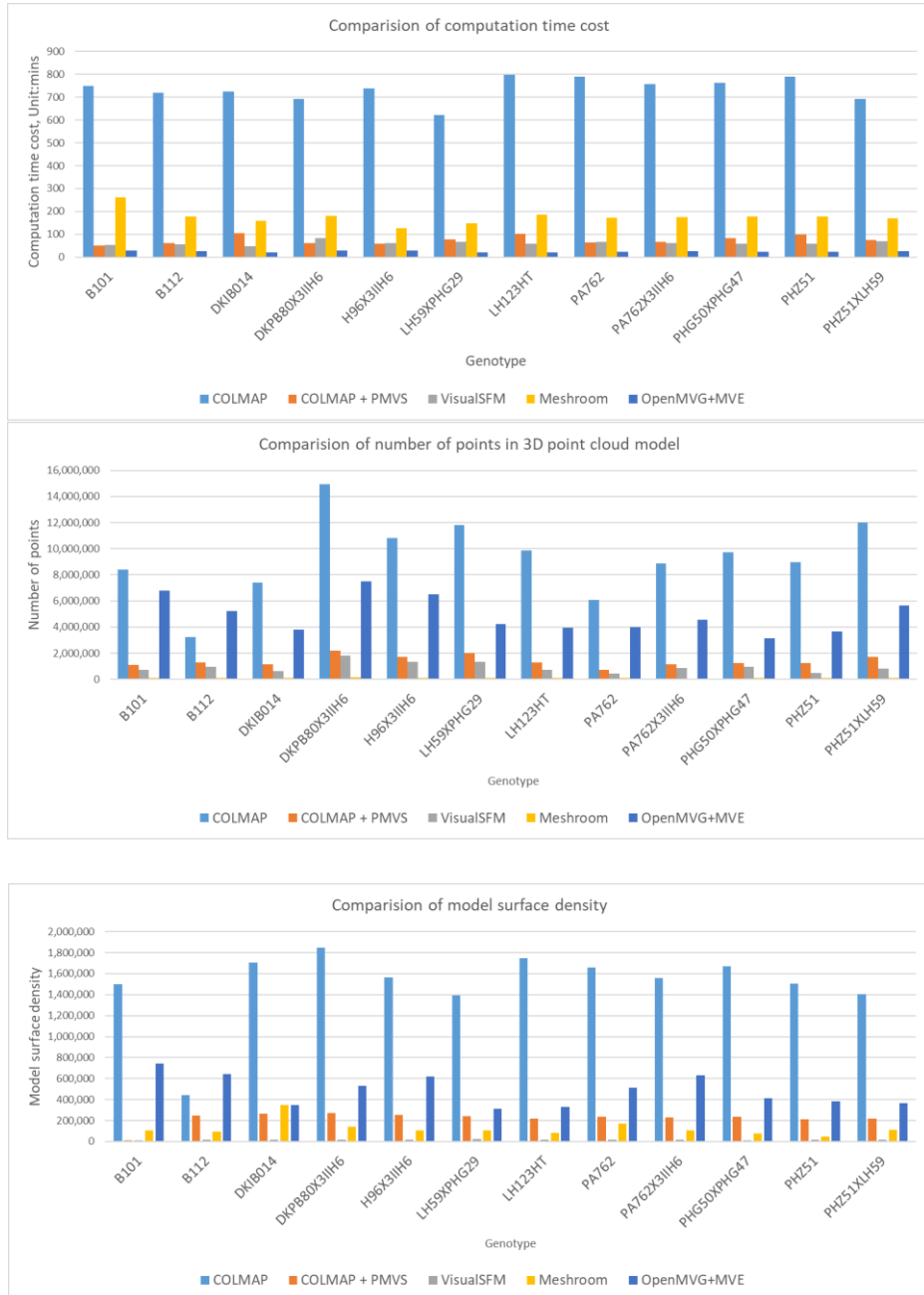


Figure 3. Comparison of time cost, number of points and surface density of 3D models

DATA AVAILABILITY STATEMENT

GitHub link for all the scripts for running the test:

https://github.com/Computational-Plant-Science/3D_review_scripts/tree/master

Cyverse link to all the 3D model results:

https://data.cyverse.org/dav-anon/iplant/home/lsx1980/3D_model_compare.zip

ACKNOWLEDGMENTS

The research was supported by the NSF CAREER Award No. 1845760 and USDOE ARPA-E ROOTS Award Number DE-AR0000821 to A.B. Any Opinions, findings, and conclusions or recommendations expressed in this material are those of the author(s) and do not necessarily reflect those of the funders.

REFERENCES

1. Schonberger, J.L. and J.-M. Frahm. *Structure-from-motion revisited*. in *Proceedings of the IEEE conference on computer vision and pattern recognition*. 2016.
2. Schönberger, J.L., et al. *Pixelwise view selection for unstructured multi-view stereo*. in *European Conference on Computer Vision*. 2016. Springer.
3. Wu, C., *VisualSfM: A visual structure from motion system*. 2011.
4. Moulon, P., et al. *Openmvg: Open multiple view geometry*. in *International Workshop on Reproducible Research in Pattern Recognition*. 2016. Springer.
5. Griwodz, C., et al. *AliceVision Meshroom: An open-source 3D reconstruction pipeline*. in *Proceedings of the 12th ACM Multimedia Systems Conference*. 2021.
6. Fuhrmann, S., F. Langguth, and M. Goesele. *MVE-A Multi-View Reconstruction Environment*. in *GCH*. 2014. Citeseer.
7. Liu, S., et al., *DIRT/3D: 3D root phenotyping for field-grown maize (Zea mays)*. *Plant Physiology*, 2021. **187**(2): p. 739-757.
8. Ault, T.R., *On the essentials of drought in a changing climate*. *Science*, 2020. **368**(6488): p. 256-260.
9. Lynch, J.P. and T. Wojciechowski, *Opportunities and challenges in the subsoil: pathways to deeper rooted crops*. *Journal of Experimental Botany*, 2015. **66**(8): p. 2199-2210.
10. Lynch, J.P., *Root phenotypes for improved nutrient capture: an underexploited opportunity for global agriculture*. *New phytologist*, 2019. **223**(2): p. 548-564.
11. Smith, P., et al., *Greenhouse gas mitigation in agriculture*. *Philosophical transactions of the royal Society B: Biological Sciences*, 2007. **363**(1492): p. 789-813.
12. Paustian, K., G. Agren, and E. Bosatta, *Modelling litter quality effects on decomposition and soil organic matter dynamics*. *Driven by nature: plant litter quality and decomposition*, 1997.
13. Dowd, T., et al., *Rated-M for mesocosm: allowing the multimodal analysis of mature root systems in 3D*. *Emerging Topics in Life Sciences*, 2021. **5**(2): p. 249.
14. Das, A., et al., *Digital imaging of root traits (DIRT): a high-throughput computing and collaboration platform for field-based root phenomics*. *Plant methods*, 2015. **11**(1): p. 1-12.
15. Delory, B.M., et al., *archiDART: an R package for the automated computation of plant root architectural traits*. *Plant and Soil*, 2016. **398**(1-2): p. 351-365.
16. Shahzad, Z., et al., *EZ-Root-VIS: a software pipeline for the rapid analysis and visual reconstruction of root system architecture*. *Plant physiology*, 2018. **177**(4): p. 1368-1381.

17. Galkovskyi, T., et al., *GiA Roots: software for the high throughput analysis of plant root system architecture*. BMC plant biology, 2012. **12**(1): p. 116.
18. Seethepalli, A., et al., *RhizoVision crown: an integrated hardware and software platform for root crown phenotyping*. Plant Phenomics, 2020. **2020**.
19. Zeng, D., et al., *TopoRoot: A method for computing hierarchy and fine-grained traits of maize roots from X-ray CT images*. bioRxiv, 2021.
20. Bucksch, A., *A practical introduction to skeletons for the plant sciences*. Applications in plant sciences, 2014. **2**(8): p. 1400005.
21. Clark, R.T., et al., *Three-dimensional root phenotyping with a novel imaging and software platform*. Plant physiology, 2011. **156**(2): p. 455-465.
22. Topp, C.N., et al., *3D phenotyping and quantitative trait locus mapping identify core regions of the rice genome controlling root architecture*. Proceedings of the National Academy of Sciences, 2013. **110**(18): p. E1695-E1704.
23. Symonova, O., C.N. Topp, and H. Edelsbrunner, *DynamicRoots: a software platform for the reconstruction and analysis of growing plant roots*. PLoS One, 2015. **10**(6): p. e0127657.
24. Stathopoulou, E.K. and F. Remondino. *Open-source image-based 3D reconstruction pipelines: Review, comparison and evaluation*. in *6th International Workshop LowCost 3D-Sensors, Algorithms, Applications*. 2019.
25. Shi, X., et al. *RootRobot: A Field-based Platform for Maize Root System Architecture Phenotyping*. in *2019 ASABE Annual International Meeting*. 2019. American Society of Agricultural and Biological Engineers.
26. Lowe, G., *Sift-the scale invariant feature transform*. Int. J, 2004. **2**(91-110): p. 2.
27. Wu, C., et al. *Multicore bundle adjustment*. in *CVPR 2011*. 2011. IEEE.
28. Wu, C. *Towards linear-time incremental structure from motion*. in *2013 International Conference on 3D Vision-3DV 2013*. 2013. IEEE.
29. Furukawa, Y. and J. Ponce. *Accurate, dense, and robust multi-view stereopsis (PMVS)*. in *IEEE Computer Society Conference on Computer Vision and Pattern Recognition*. 2007.
30. Zheng, E., et al. *Patchmatch based joint view selection and depthmap estimation*. in *Proceedings of the IEEE Conference on Computer Vision and Pattern Recognition*. 2014.
31. Alcantarilla, P.F. and T. Solutions, *Fast explicit diffusion for accelerated features in nonlinear scale spaces*. IEEE Trans. Patt. Anal. Mach. Intell, 2011. **34**(7): p. 1281-1298.
32. Muja, M. and D.G. Lowe, *Fast approximate nearest neighbors with automatic algorithm configuration*. VISAPP (1), 2009. **2**(331-340): p. 2.
33. Cheng, J., et al. *Fast and accurate image matching with cascade hashing for 3d reconstruction*. in *Proceedings of the IEEE Conference on Computer Vision and Pattern Recognition*. 2014.
34. Goesele, M., B. Curless, and S.M. Seitz. *Multi-view stereo revisited*. in *2006 IEEE Computer Society Conference on Computer Vision and Pattern Recognition (CVPR'06)*. 2006. IEEE.
35. Hirschmuller, H., *Stereo processing by semiglobal matching and mutual information*. IEEE Transactions on pattern analysis and machine intelligence, 2007. **30**(2): p. 328-341.
36. Girardeau-Montaut, D., *CloudCompare*. France: EDF R&D Telecom ParisTech, 2016.